J Ind Microbiol Biotechnol (2011) 38:975–983
DOI 10.1007/s10295-010-0870-y

ORIGINAL PAPER

Role of supramolecular cellulose structures in enzymatic hydrolysis of plant cell walls

Lisbeth Garbrecht Thygesen · Budi Juliman Hidayat · Katja Salomon Johansen · Claus Felby

Received: 30 May 2010 / Accepted: 31 August 2010 / Published online: 18 September 2010

Abstract The study of biomass deconstruction by enzymatic hydrolysis has hitherto not focussed on the importance of supramolecular structures of cellulose. In lignocellulose fibres, regions with a different organisation of the microfibrils are present. These regions are called dislocations or slip planes and they are known to be more susceptible to various forms of degradation such as acid hydrolysis. Traditionally the cellulose within these regions has been assumed to be amorphous, but in this study it is shown by use of polarized light microscopy that dislocations are birefringent. This indicates that they have a crystalline organisation. Dislocations may be entry points for endoglucanases. Using a fluorescent labelled endoglucanase combined with confocal fluorescence microscopy, it is shown that the enzyme selectively binds to dislocations during the initial phase of the hydrolysis. Using a commercial cellulase mixture on hydrothermally treated wheat straw, it was found that the fibres were cut into segments corresponding to the sections between the dislocations initially present, as has previously been observed for acid hydrolysis of softwood pulps. The results indicate that dislocations are important during the initial part of enzymatic hydrolysis of cellulose. The implications of this phenomenon have not yet been recognized or explored within cellulosic biofuels.

Keywords Dislocations · Slip planes · Enzymatic hydrolysis · Supramolecular structures of cellulose · Cellulosic biofuels

This article is based on a presentation at the 32nd Symposium on Biotechnology for Fuels and Chemicals.

L. G. Thygesen (✉) · B. J. Hidayat · C. Felby
Forest and Landscape, Faculty of Life Sciences,
University of Copenhagen, Rolighedsvej 23,
1958 Frederiksberg C, Denmark
e-mail: lgt@life.ku.dk

K. S. Johansen
Novozymes A/S, Krogshøjvej 36, 2880 Bagsværd, Denmark

Introduction

The structure of cellulose within secondary plant cell walls has been studied for decades and native cellulose is presently considered as being either I_α or I_β crystals [3]. The structure of cellulose on the supramolecular level has received less attention in relation to biomass recalcitrance and cellulosic bioethanol production. This study focuses on the role of supramolecular structures known as dislocations in the enzymatic degradation of lignocellulose.

Supramolecular structures now known as dislocations, slip planes or nodes [26] have been known for more than 100 years. They have been observed not only in wood [29], but also in bast fibres, for example in hemp [5, 33–36], flax [4–7] and nettle [5, 7]. Dislocations may be induced either by mechanical action on the fibres/tracheids after harvest (compression in the longitudinal direction of the cell [9, 32]) or may already be present in the plant at harvest [34]. The reason for their occurrence in the living plant is unknown but has also been assumed to be caused by mechanical action (wind leading to longitudinal compression within the lee side of the plant). In accordance with this theory more dislocations have been found in hemp plants subjected to wind [34]. However, since drought also induces dislocations, growth stress during biosynthesis of microfibrils is another possible cause [34]. Since both these

causes may affect the cellulose microfibrils in the cell walls of thick-walled cells within supporting tissues of higher plants regardless of species, it is likely that dislocations are a generic phenomenon that occurs in many higher plants in spite of differences in cell wall structure. Furthermore, dislocations found in one species are likely to be similar to those found in other species.

Research concerning dislocations has hitherto been done within pulp and paper science, and has been directed towards the detrimental effects of dislocations on paper and fibre strength properties [9, 32] or on exploring where in the pulping process dislocations are formed [10, 14, 21, 25, 27]. Since dislocations have been found to reduce paper strength and to be more susceptible to acid hydrolysis [1], the cellulose within dislocations has been assumed to be amorphous in contrast to the crystalline bulk cell wall. Recently, Kawakubo et al. [20] reported results which seem to strengthen this hypothesis. They investigated the binding of two different carbohydrate binding modules (CBMs) to cedar wood pulps. *Clostridium josui* CBM28, a CBM known to target isolated saccharide chains (interpreted as amorphous cellulose), was found to bind to delignified fibre surfaces at certain regions. Kawakubo and co-workers interpreted these regions as amorphous cellulose on the fibre surface exposed by bending or physical stress during the delignification process. To the present authors these regions appear to be identical to dislocations. *Clostridium josui* CBM3, a CBM known to bind to flat surfaces of crystalline cellulose, did not show this tendency. On the other hand Filonova et al. [13] found increased amounts of labelled CBM1 from *Hypocrea jecorina* (identical to *Trichoderma reesei*) Cel7A in dislocations in spruce pulp fibres as well as in other sites where the fibres were damaged. Filonova et al. [13] stated that this CBM binds exclusively to crystalline cellulose. Perhaps the conflicting results illustrate that the microstructure of plant cell walls is more complex than what may be revealed by using probes whose binding properties have been characterised based on isolated cellulose substrates.

Ander et al. [1] developed a method for quantification of the amount of dislocations within pulp. The method is based on acid hydrolysis of pulp fibres under standardized conditions (i.e. acidity, time span, temperature and stirring) followed by a measurement of the length distribution of the fibre segments using automatic image analysis. The premise is that the pulp fibres will break in dislocations during the hydrolysis step, i.e. the more 'short' fibre segments and the fewer 'long' fibre segments present after hydrolysis, the more dislocations were present from the beginning. Thygesen [33] proved the premise to be correct and also confirmed that strict standardisation of the method is necessary as many dislocations are still present in the fibre segments after the acid hydrolysis step.

A few studies have suggested that dislocations are more susceptible than the surrounding bulk cell wall not only to acid hydrolysis but also to enzymatic hydrolysis. It is not obvious that this should be the case, as the small acid molecules presumably more easily penetrate into the cell wall. Hildén et al. [15] labelled the CBM from *Phanerochaete chrysosporium* cellulase Cel7D, and found that it bound more to 'hot spots located at fibre kinks or damaged areas', i.e. to the supramolecular structures denoted dislocations. Ander et al. [2] compared acid (HCl) and enzymatic hydrolysis of pulp fibres using a variety of monocomponent cellulases and cellulase mixtures (EGII and CBHI from *Trichoderma reesei*, Novozym 476, Novozym 342, N342 and Celluclast). The focus of these studies was to identify hydrolysis systems that gave different results for pulps based on different sources of wood and prepared in different ways. The results were compared based on an estimate of the average number of cleavages per fibre during hydrolysis. Segmentation of fibres was seen for all enzyme treatments reported, but results may not be compared between enzymes due to differences in treatment times and enzyme doses. Also, to the present authors the results presented by Ander et al. [2] indicate that the estimate of the number of cleavages per fibre to some extent depends on the average fibre length prior to hydrolysis, which prohibits comparison between results based on different pulps. In another study, Suchy et al. [31] measured the zero-span wet strength of bleached hardwood kraft pulp after treatment with a commercial enzyme product based on a family Cel7A CBH from *Thermoascus aurantiacus*. They observed straighter and cleaner fractures and more cracks in the fibre surfaces after enzyme treatment and interpreted this as the result of the localized action of the enzyme at dislocations.

In the present study the objective was to explore the structure of dislocations and their role in enzymatic hydrolysis of hydrothermally treated wheat straw under industrial-like conditions. In particular, we wished to employ automatic image analysis of fibre length and width in order to follow the development in fibre dimensions during hydrolysis and liquefaction of lignocellulose.

Materials and methods

Hydrothermally treated wheat straw

Wheat straw (*Triticum aestivum*) was pretreated by using the IBUS cellulosic ethanol facility [23]. The straw is cut into 50-mm segments, soaked for 5 min at 80°C and run through a hydrothermal reactor at 190°C for 12 min. After pretreatment the straw contains 59% cellulose, 5% hemicellulose and 25% lignin. The dry matter of the pretreated straw is approximately 25% and pH 4.5. Fibres are the

dominant cell type of the pretreated straw. The treated straw was a gift from the company Inbicon (Kalundborg, Denmark, http://www.inbicon.com). Further data on the structure and composition of the straw can be found in [22].

Enzymatic hydrolysis

Hydrolysis of the pretreated straw was carried out by using a 5:1 mixture of Celluclast and Novozym 188 at 5 FPU (fibre paper units) per gram dry matter. The enzymes were a gift from the company Novozymes A/S (Bagsværd, Denmark, http://www.novozymes.com). The enzymes were added to the pretreated straw together with a pH 4.8 sodium citrate buffer. Each sample contained 12.5 g pretreated straw (dry matter). The dry matter content of the mixture (pretreated straw + buffer + enzymes) was 25%, and the temperature during the hydrolysis was 50°C. The high dry matter content implies that at the onset of hydrolysis, all liquid was adsorbed by the substrate [12]. The samples were subjected to free fall mixing during the hydrolysis. Free fall mixing is done by using a rotating horizontal mixer [18]. In the present experiment free fall mixing implied that hydrolysis was carried out in 100-ml plastic bottles placed in an 800-mm-diameter horizontal drum rotating at 60 rpm. The drum was equipped with two paddles that lifted and dropped the bottles during rotation. Samples (duplicates) were taken out after 0, 1, 2, 3, 4, 6 and 24 h of hydrolysis. Two different controls were also run in duplicates: (1) free fall mixing only, i.e. the same conditions during hydrolysis as for the time series, but only buffer was added to the pretreated straw (i.e. no enzymes added); and (2) enzymes only, i.e. the samples were identical to the samples used for the time series, but in contrast to these they were not subjected to any mixing. Both types of controls were run for 24 h at 50°C. Hydrolysis was stopped by boiling the samples in water for 10 min. Samples were then stored in a refrigerator at +4°C for a few days before fibre length and width analysis.

Polarized light microscopy (PLM)

PLM was carried out by using a Zeiss Axioplan microscope equipped with two polarisers, a rotating stage and a Pixelink digital camera.

Fluorescent labelling, confocal laser scanning microscopy (CLSM) and pseudo PLM

The fluorescence labelling procedure was a slightly modified version of the one recommended by the manufacturer. An endoglucanase (family GH45 from *Humicola insolens*, here denoted enzyme A) was obtained in a chromatographically pure form from Novozymes, Bagsværd, Denmark. More information on this enzyme and details of its preparation can be found in [11]. After incubation of the enzyme with DyLight 633™ (Thermo Scientific, Rockford, IL, USA) for 1 h (standing) in 0.05 M pH 8.5 borate buffer at room temperature, excess fluorophore was removed by centrifugation (4,700 rpm, 15 min, multiple times, until a clear supernatant solution was obtained) using a Vivaspin ultrafiltration spin column (5 K MWCO, Sartorius Stedim GmbH, Goettingen, Germany). A fluorophore to protein ratio (in mol basis) of 1.4:1 was obtained.

Samples for CLSM were prepared by spotting 40 µl labelled enzyme solution (10^{-5} M) onto Filtrak filter paper fibres (Munktell and Filtrak GmbH, Bärenstein, Germany), which had been isolated by hand using precision tweezers and placed on a glass slide. After 10 min a cover slip was applied and the slide was observed by using a confocal microscope [Leica TCS SP2, Leica Microsystems using a ×63 objective (NA 1.2)]. Excitation was performed by using a 633-nm laser at 20% laser power and emission was collected for the 650–800-nm range. Images were colour-coded according to the intensity of the light emission within this interval, going from black (no emission) over brownish-reddish to yellow and white (maximum emission). Blue coding signalled detector overload.

In order to acquire pseudo PLM images of the exact same scene as the one captured by using CLSM, the transmission detector of the confocal microscope was used. A 488-nm laser was employed as light source, and crossed polars were inserted in the pathway of the laser beam before and after the sample (polarization of laser light ought to be redundant, but nevertheless a better image quality was experienced).

The images were not subjected to any image processing except for the pseudo PLM images, for which the distribution of grey-scale values occurring in the image was expanded to the full interval (0–255). This procedure increased contrast.

Environmental scanning electron microscopy (ESEM)

ESEM was carried out by using a FEI Quanta 200. Images were obtained for uncoated samples in low vacuum mode using an X-ray cone (voltage 20 kV, pressure 110–130 Pa). The images were not subjected to any image processing.

Fibre length and width analysis

Automatic image analysis of fibre dimensions based on the FiberTester system was carried out by the company Innventia (Stockholm, Sweden, http://www.innventia.se). The FiberTester is a new version of the FiberMaster instrument. The instrument was developed for the pulp and paper industry, and has to the best of the authors' knowledge not

been tested earlier for monitoring enzymatic hydrolyses of wheat straw. The FiberTester gives information on fibres and fibre segments regarding length, width and form factor (a number between 0 and 100 indicating how straight or curled a fibre is). The method is based on automatic image analysis of micrographs of fibres and/or fibre segments suspended in water and run in a closed loop. A sample consists of 0.5 g dry matter suspended in 500 ml of water. For each sample, analysis stops when about 100,000 objects have been measured. The standard output from the FiberTester analysis is only based on particles that fulfil certain fibre criteria [19, 33]. In the present case the fibre criteria were not employed. Results reported here are based on all particles with a length equal to at least 13 µm (the detection limit), and a positive form factor not larger than 100 (a form factor outside this interval signals an erroneous measurement).

Results and discussion

Crystallinity of bulk cell wall and dislocations

Crystalline cellulose is birefringent. This implies that when a cellulose microfibril is placed under crossed polars and the microscope stage is rotated, the fibril will disappear, i.e. it will appear black when the longitudinal direction of the microfibril is parallel to the polarization direction of one of the two filters. This phenomenon is denoted extinction. At the four positions shifted 45° relative to the extinction positions, the fibril lights up, i.e. maximal brightness is obtained. A plant cell wall which contains an S2 layer is also birefrigent, and because birefringence is additive, a plant fibre will behave just like a single fibril no matter which microfibril angle (MFA) the microfibrils in the S2 layer have, as the MFA of the microfibrils in the upper wall is cancelled out by the mirrored MFA of the microfibrils in the lower wall, so that the average MFA is 0°. The four positions corresponding to extinction and the four positions corresponding to maximum brightness are shown for the bulk cell wall of a filter paper fibre (softwood tracheid) in Fig. 1. The fibre contains dislocations, and for the four extinction images they are visible (oblong bright areas across the fibre), as their MFA is not cancelled out by opposite orientations in the lower side of the fibre. However, Fig. 2 shows that a dislocation behaves exactly like the bulk cell wall; extinction and maximum brightness just appear for different positions of the fibre. This implies that dislocations are birefringent and thus appear to be crystalline. In other words Figs. 1 and 2 indicate that dislocations are not amorphous contrary to what has hitherto been assumed.

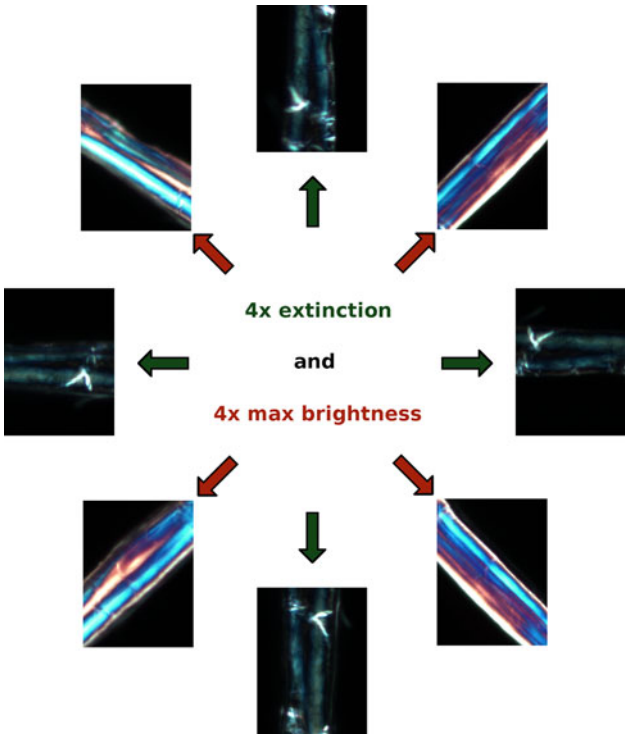

Fig. 1 Bulk cell wall: PLM images of a filter paper fibre (softwood tracheid) rotated to different angles relative to the vibrational direction of the two polarization filters. When the longitudinal direction of the fibre is parallel to one of the two filters (*green arrows*), the light is extinct. At the four positions rotated 45° away from the extinction positions (*red arrows*), maximum brightness is seen

Cellulase adsorption to dislocations

Figures 3 and 4 show the corresponding pseudo PLM and CLSM images of two different plant cells spotted with enzyme A. Figure 3 shows a filter paper tracheid, and Fig. 4 shows a pretreated wheat straw fibre cell; in both cases the endoglucanase is seen to have a preference for dislocations. This is the first time CLSM and PLM has been combined and in situ shown preference for dislocations of an endoglucanase. Earlier results have indicated preference for dislocations of CBMs [13, 15, 20] or different glucanases [2], but without direct in situ PLM visualisation of the dislocations. That the same pattern is seen for both cell types strengthens the hypothesis given in the "Introduction" that dislocations are a generic phenomenon present in different plant species in spite of differences in cell wall structure.

The reason for the observed preference of enzyme A for dislocations is not known. Figure 2 shows that it is not reasonable to claim that the susceptibility of dislocations to hydrolysis is due to the presence of amorphous cellulose. In addition, a recent study led to the conclusion that cellulose digestibility cannot be explained solely by its crystallinity

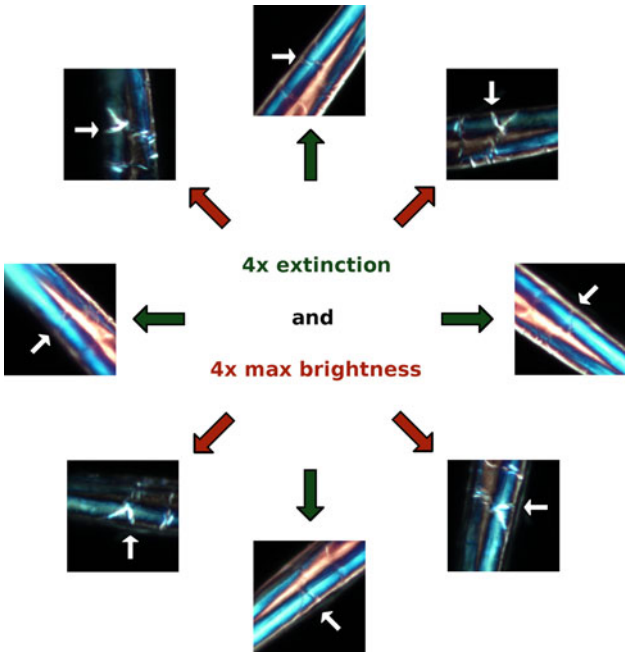

Fig. 2 Dislocation: PLM images of a filter paper fibre (softwood tracheid) rotated to different angles relative to the vibrational direction of the two polarization filters. When the longitudinal direction of the microfibrils within the dislocation (*white arrows*) is parallel to one of the two filters (*green arrows*), the light is extinct. At the four positions rotated 45° away from the extinction positions (*red arrows*), maximum brightness is seen

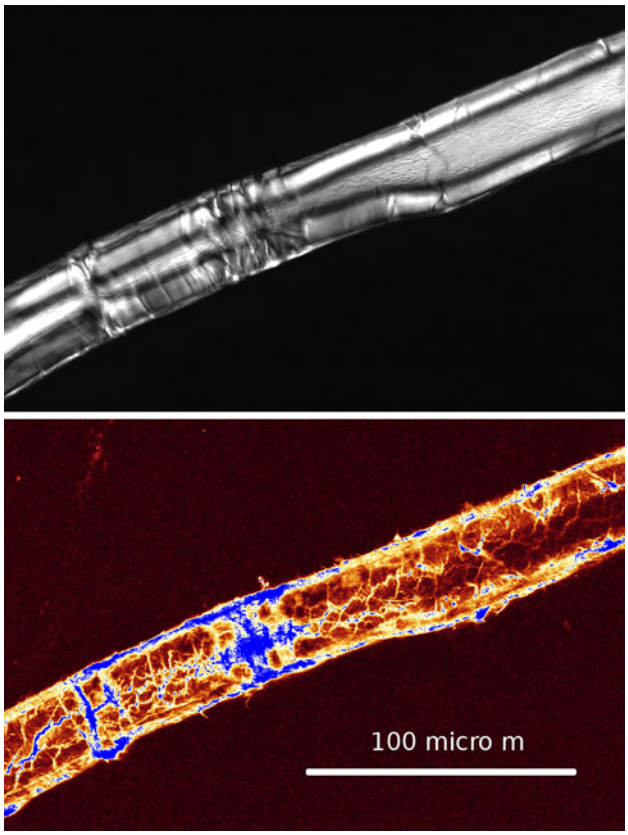

Fig. 3 Pseudo PLM and CLSM images of a filter paper fibre (softwood tracheid) spotted with fluorescent labelled enzyme A (an endoglucanase). The enzyme is seen to bind strongly to the two dislocations

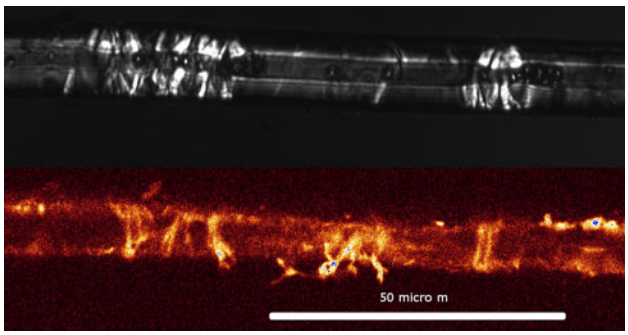

Fig. 4 Pseudo PLM and CLSM images of a pretreated wheat straw fibre spotted with fluorescent labelled enzyme A (an endoglucanase). The enzyme is seen to bind to the two dislocations and to loosened fibrils

index, also accessibility plays a role [28]. Minute cracks and/or a 'loosening' of the structure in dislocations might in this way be a factor contributing to the observations in Figs. 3 and 4, i.e. the increased presence of enzymes in the dislocations may perhaps to some extent be caused by capillary forces. Another hypothesis could be that it has to do with possible differences in cellulose crystal structure. Recently, Santa-Maria and Jeoh [30] observed untwisting of cellulose microfibrils during hydrolysis of never-dried Cellulose I using a purified cellobiohydrolase. One can speculate that microfibrils are less twisted within dislocations, making the microfibrils more accessible to hydrolysis while retaining the birefringence of the cell wall.

Fibres are cut into segments at the dislocations during enzymatic hydrolysis

Figure 5 shows the total length and width of about 100,000 particles measured for each of the samples taken out during the enzymatic hydrolysis experiment for hydrothermally treated wheat straw. Figure 5 shows that the total length of the first 100,000 particles encountered during FiberTester analysis gradually decreases to about 50% of the original value, while the total width of the same particles only is reduced by about 10%. This shows that fibres are cut into segments during hydrolysis. None of the two control treatments had any significant effects compared to the length and width data at the onset of hydrolysis. A more detailed account of the development in particle dimensions during enzymatic hydrolysis is given in Fig. 6. Figure 6a shows the amount of particles within different length ranges given as percentages of the total length of all 100,000 particles measured within that sample (i.e. as percentages of the lengths shown in Fig. 5). Since the number of short fibres increased dramatically during hydrolysis compared to the corresponding

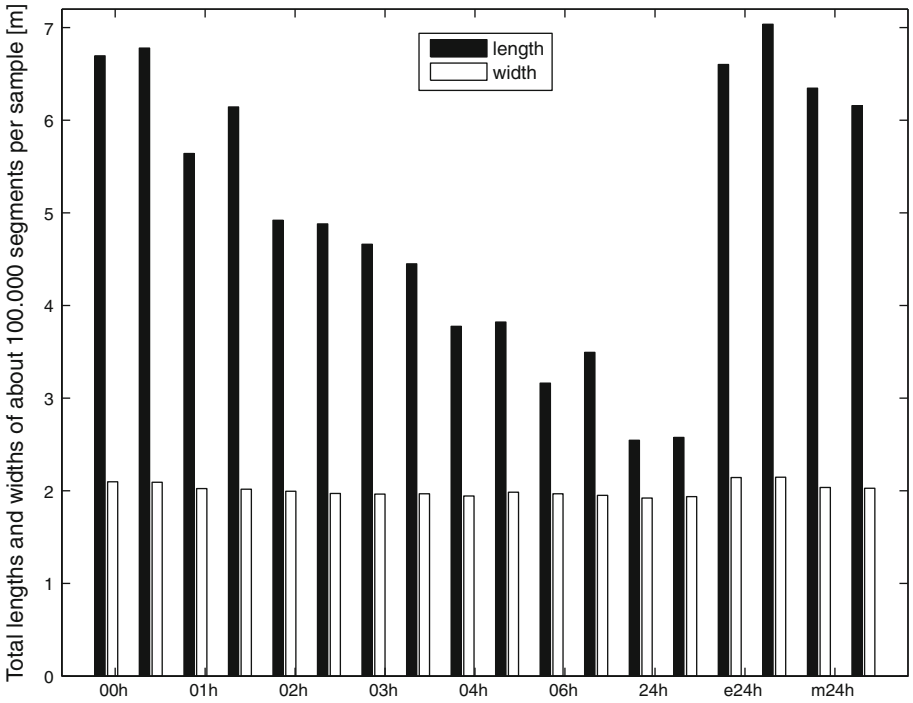

Fig. 5 FiberTester results for hydrothermally treated wheat straw during hydrolysis, shown as total lengths and total widths. Results are shown in duplicates. The *four last columns* are the two controls, *e24* is 'enzyme only', *m24* is 'mixing only'

decrease in the number of long fibres, these length-weighted distributions are shown instead of distributions based on the number of particles within the various length classes. Figure 6a shows that during the first hours of hydrolysis most of the long fibre segments (longer than 2–300 µm) are broken into medium length segments, while further segmentation into the final 20–40 µm segments continues into the later stages of the hydrolysis. The amount of particles in the 80–200 µm range increased up to 6 h, thereafter a slight (80–100 µm) or a more substantial (100–200 µm) decrease was seen. The amount of particles shorter than 60 µm increased throughout the experiment, especially for the particles with lengths in the 20–40 µm range. Regarding length to width ratios, Fig. 6b shows that during hydrolysis, particles longer than four times their width were cut into pieces with ratios only slightly over one. The amount of particles with intermediate ratios remained low and more or less constant throughout the hydrolysis experiment. The overall picture shows that oblong particles with aspect ratios above four are cut into almost square particles during hydrolysis. Also, it appears that the liquefaction process (i.e. the first 6 h of enzymatic hydrolysis) is characterized by a decrease in the amount of particles above 200–300 µm length and a corresponding increase in the amount of particles shorter than 80 µm length, especially the 20–40 µm range, while a decrease in the amount of particles with intermediate lengths (80–200 µm) mainly sets in after the substrate has become liquefied.

The results presented in Figs. 5 and 6 show the potential of FiberTester analysis for monitoring enzymatic hydrolysis of biomass. For example, detailed knowledge of the development in particle dimensions during the liquefaction step can be obtained and used within design and development of more energy efficient mixing regimes for industrial production of cellulosic biofuels.

Previous studies of the enzymatic hydrolysis of plant fibres have shown that the hydrolysis starts at the surface of the wall when no mixing is applied [8]. The surface erosion model for the action of one of the most important enzymes in the Celluclast product, the cellobiohydrolase Cel7A, is well established [16, 17, 24] but the FiberTester results presented here show that on the whole cell scale, initial enzymatic hydrolysis is transversal rather than longitudinal.

Figure 7 shows ESEM images of the hydrothermally treated wheat straw after 24 h of hydrolysis and free fall mixing, and after 24 h of free fall mixing only. The images show that the particles seen after hydrolysis are short and have smooth, sharp ends ('scissor-cut' ends), while the particles seen after mixing only are long and have torn ends. These differences show that while the combination of cellulolytic enzymes and free fall mixing results in a cutting of fibres into particles, the mechanical process of free fall mixing only results in fibrillation at the ends of the fibres. Together with Figs. 5 and 6 this shows that it is not the mixing per se that gives fibre shortening, and that only the combined action of enzymatic hydrolysis and free fall mixing results in clean-cut fibre segments.

Figure 8 shows PLM images of hydrothermally pretreated wheat straw fibres before and after 24 h of enzymatic hydrolysis and free fall mixing. The image in Fig. 8a shows a typical fibre cell prior to hydrolysis. Dislocations are seen to be present, and the image indicates that the

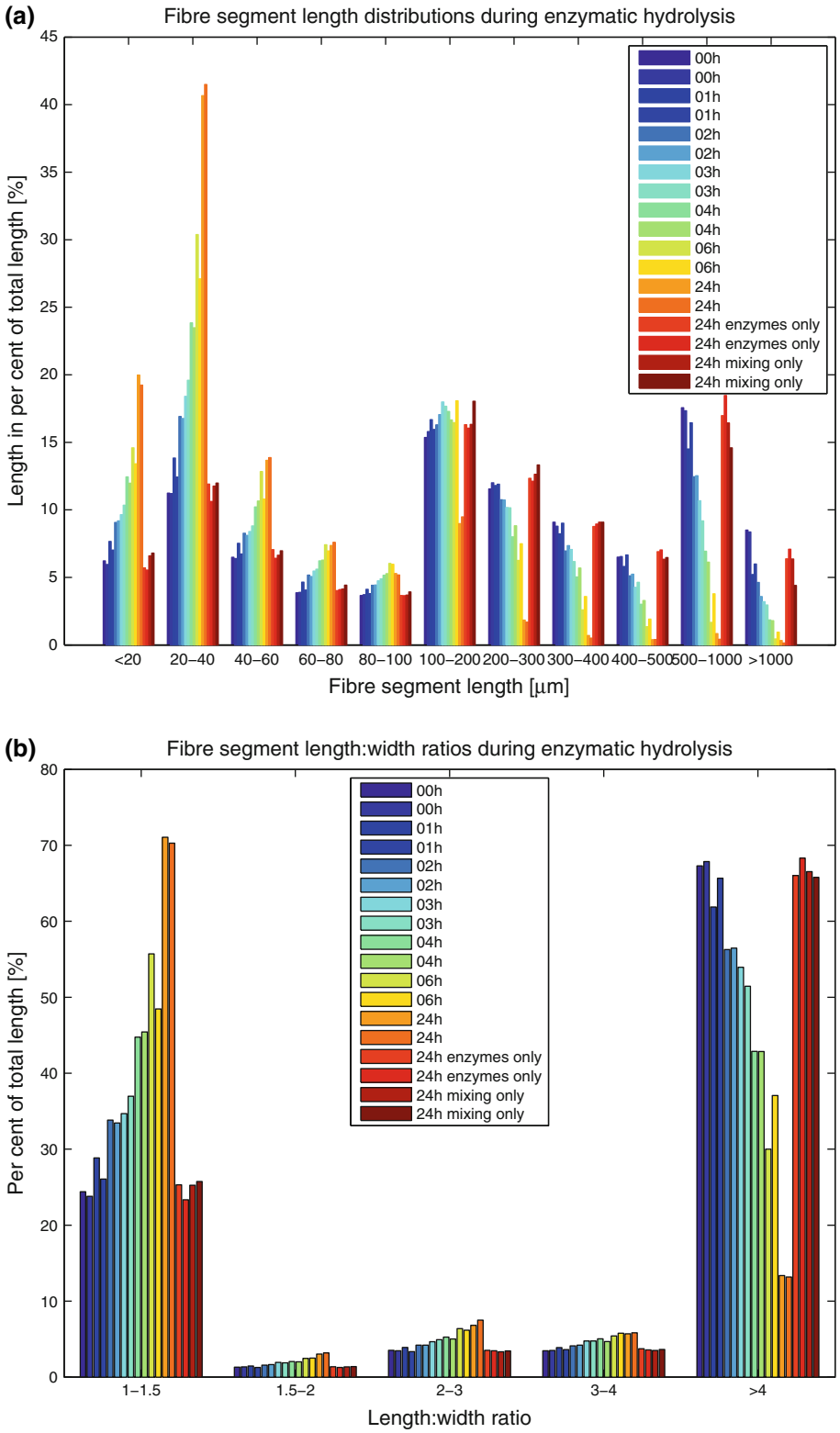

Fig. 6 FiberTester results for hydrothermally treated wheat straw during hydrolysis. Results are shown in duplicates. **a** Total length of all particles encountered within the specified length intervals in per cent of the total length of all particles measured for the sample. **b** Distribution of particles into ranges of length to width ratios (aka aspect ratios). Percentages given are percentages of the total length of all particles measured for the samples

typical minimum distance between large dislocations is about 20 µm, i.e. about the same distance as the dominant fibre segments after 24 h of hydrolysis (Fig. 5a). After 24 h of hydrolysis (Fig. 7b) only few and small dislocations are seen, as exemplified by this typical fibre segment. Together, Figs. 7 and 8 thus indicate that fibres are cut into segments at dislocations during hydrolysis. It should be noted that no quantitative analysis of distances between dislocations was carried out, but the typical distances between dislocations were as shown in Fig. 8.

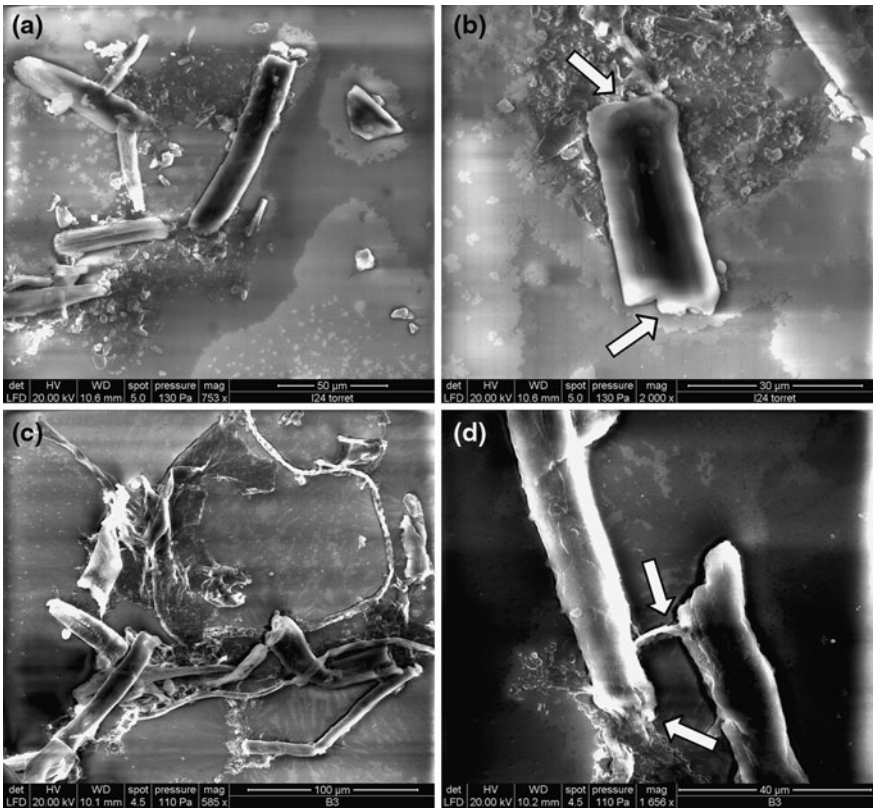

Fig. 7 ESEM images of hydrothermally treated wheat straw after 24 h of hydrolysis (**a** and **b**), and after 24 h of free fall mixing without enzymes added (**c** and **d**). Hydrolysis gave short segments with sharp, 'scissor-cut' ends; mixing resulted in long segments with torn ends. The *arrows* point to 'scissor-cut' ends (in **b**) and to torn ends (in **d**)

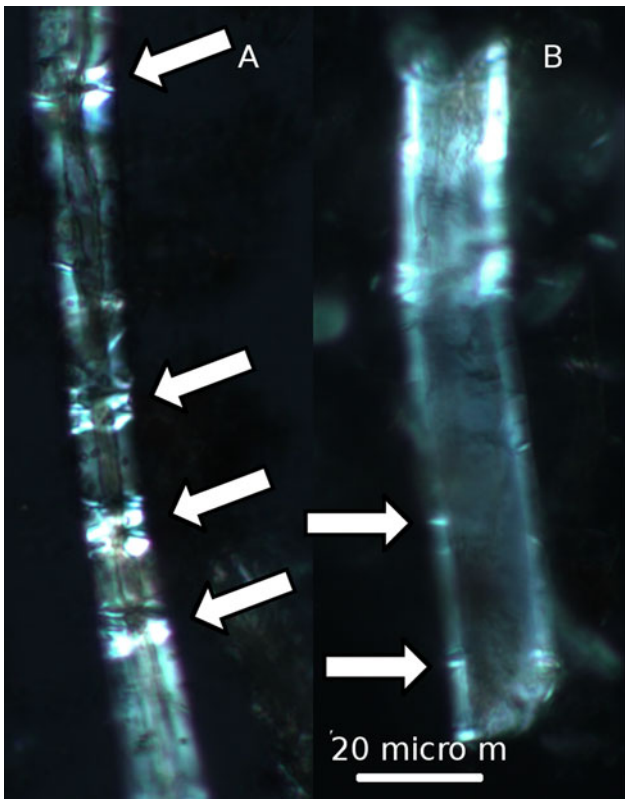

Fig. 8 PLM images of dislocations in hydrothermally treated wheat straw fibres before (**a**) and after (**b**) 24 h of hydrolysis. The *arrows* point to dislocations

Conclusions

This study concerned enzymatic hydrolysis carried out at high dry matter contents and using free fall mixing. Under these industrial-like conditions, degradation of cellulose present inside secondary plant cell walls started at dislocations and fibres broke into segments at these locations. The substrate was liquefied at the same time as the amount of segments longer than 3–400 μm was markedly reduced.

It was shown that an endocellulase preferred binding to dislocations over binding to the bulk cell wall. The reason for this is not known, but it indicates that cellulose in dislocations is more easily accessible and/or more easily degradable. However, a simple PLM experiment (Figs. 1, 2) indicated that the cellulose within dislocations is not amorphous, contrary to what has become an established assumption.

The results of the present study indicate that dislocations play an important role during the initial stages of enzymatic hydrolysis of lignocellulose under industrial conditions.

Acknowledgments The authors acknowledge Novozymes A/S for funding the work and for donating all enzymes used. CLSM was carried out at the Center for Advanced Bioimaging (CAB), University of Copenhagen, Denmark, and ESEM at the Department of Civil Engineering, Technological University of Denmark. The hydrothermally treated wheat straw was a gift from Inbicon. Innventia is thanked for giving the authors access to the raw output data from the FiberTester analysis.

References

1. Ander P, Daniel G, Garcia-Lindgren C, Marklund A (2005) Characterization of industrial and laboratory pulp fibres using HCL, cellulose and FiberMaster analysis. Nord Pulp Pap Res J 20:115–120
2. Ander P, Hildén L, Daniel G (2008) Cleavage of softwood kraft pulp fibres by HCl and cellulases. Bioresources 3(2):477–490
3. Attalla RH, VanderHart DL (1984) Native cellulose: a composite of two distinct crystalline forms. Science 223(4633):283–285
4. Baley C (2004) Influence of kink bands on the tensile strength of flax fibers. J Mater Sci 39:331–334
5. Bergfjord C, Karg S, Rast-Eicher A, Nosch M-L, Mannering U, Allaby RG, Murphy BM, Holst B (2010) Comment on "30,000-year-old wild flax fibers". Science 328:1634. doi:10.1126/science.1186345
6. Bos HL, Donald AM (1999) In situ ESEM study of the deformation of elementary flax fibres. J Mater Sci 34:3029–3034
7. Davies GC, Bruce DM (1998) Effect of environmental relative humidity and damage on the tensile properties of flax and nettle fibers. Textile Res J 68(9):623–629
8. Donohoe BS, Selig MJ, Viamajala S, Vinzant TB, Adney WS, Himmel ME (2009) Detecting cellulose penetration into corn stover cell walls by immuno-electron microscopy. Biotechnol Bioenergy 103(3):480–489. doi:10.1002/bit.22281
9. Eder M, Terziev N, Daniel G, Burgert I (2008) The effect of (induced) dislocations on the tensile properties of individual Norway spruce fibres. Holzforschung 62(1):77–81. doi:10.1515/HF.2008.011
10. Ellis MJ, Duffy GG, Allison RW, Kibblewhite RP (1997) Fibre deformation during medium consistency mixing: role of residence time and impeller geometry. Appita 2:643–649
11. Eriksson J, Malmsten M, Tiberg F, Callisen TH, Damhus T, Johansen KS (2005) Model cellulose films exposed to *H. insolens* glucoside hydrolase family 45 endo-cellulase—the effect of the carbohydrate-binding module. J Colloid Interface Sci 285:94–99. doi:10.1016/j.jcis.2004.10.042
12. Felby C, Thygesen LG, Kristensen JB, Jørgensen H, Elder T (2008) Cellulose-water interactions during enzymatic hydrolysis as studied by time domain NMR. Cellulose 15:703–710. doi:10.1007/s10570-008-9222-8
13. Filonova L, Kallas ÅM, Greffe L, Johansson G, Teeri TT, Daniel G (2007) Analysis of the surfaces of wood tissues and pulp fibers using carbohydrate-binding modules specific for crystalline cellulose and mannan. Biomacromolecules 8:91–97. doi:10.1021/bm060632z
14. Hakanen A, Hartler N (1995) Fiber deformations and strength potential of kraft pulps. Paperi ja Puu 77(5):339–344
15. Hildén L, Daniel G, Johansson G (2003) Use of a fluorescence labelled, carbohydrate-binding module from *Phanerochaete chrysosporium* Cel7D for studying wood cell wall ultrastructure. Biotechnol Lett 25:553–558
16. Igarashi K, Koivula A, Wada M, Kimura S, Penttilä M, Samejima M (2009) High-speed atomic force microscopy visualizes processive movement of *Trichoderma Reesei* cellobiohydrolase I on crystalline cellulose. J Biol Chem 284(52):36186–36190. doi:10.1074/jbc.M109.034611
17. Imai T, Boisset C, Samejima M, Igarashi K, Sugiyama J (1998) Unidirectional processive action of cellobiohydrolase Cel7A on *Valonia* cellulose microcrystals. FEBS Lett 432:113–116
18. Jørgensen H, Vibe-Pedersen J, Larsen J, Felby C (2007) Liquefaction of lignocellulose at high-solids concentrations. Biotechnol Bioeng 5:862–870. doi:10.1002/bit
19. Karlsson H, Franson P-I, Mohlin U-B (1999) STFI fiberMaster. In: Proceedings from the 6th international conference on new available technologies, SPCI, pp 367–374
20. Kawakubo T, Karita S, Araki Y, Watanabe S, Oyadomari M, Takada R, Tanaka F, Abe K, Watanabe T, Honda Y, Watanabe T (2010) Analysis of exposed cellulose surfaces in pretreated wood biomass using carbohydrate-binding module (CBM)-cyan fluorescent protein (CFP). Biotechnol Bioeng 105(3):499–507. doi:10.1002/bit.22550
21. Kibblewhite RP (1976) Fractures and dislocations in the walls of kraft and bisulphite pulp fibres. Cellulose Chem Technol 10:497–503
22. Kristensen JB, Thygesen LG, Felby C, Jørgensen H, Elder T (2008) Cell-wall structural changes in wheat straw pretreated for bioethanol production. Biotechnol Biofuels 1:5. doi:10.1186/1754-6834-1-5
23. Larsen J, Petersen MØ, Thirup L, Li HW, Iversen FK (2008) The IBUS process—lignocellulosic bioethanol close to commercial reality. Chem Eng Technol 31(5):765–772. doi:10.1002/ceat.200800048
24. Lehtiö J, Sugiyama J, Gustavsson M, Fransson L, Linder M, Teeri TT (2003) The binding specificity and affinity determinants of family 1 and family 3 cellulose binding modules. PNAS 100(2):484–489. doi:10.1073/pnas.212651999
25. Mohlin U-B, Alfredsson C (1990) Fibre deformations and its implications in pulp characterization. Nord Pulp Paper Res J 4:172–179
26. Nyholm K, Ander P, Bardage S, Daniel G (2001) Dislocations in pulp fibres—their origin, characteristics and importance—a review. Nord Pulp Pap Res J 4(16):376–384
27. Page DH (1966) The axial compression of fibers—a newly discovered beating action. Pulp Paper Mag Can T2–T12
28. Park S, Baker JO, Himmel ME, Parilla PA, Johnson DK (2010) Cellulose crystallinity index: measurement techniques and their impact on interpreting cellulose performance. Biotechnol Biofuels 3:10. doi:10.1186/1754-6834-3-10
29. Robinson W (1920) The microscopical features of mechanical strains in timber and the bearing of these on the structure of the cell-walls in plants. Philos Trans R Soc Lond B Biol Soc 210:49–82
30. Santa-Maria M, Jeoh T (2010) Molecular-scale investigations of cellulose microstructure during enzymatic hydrolysis. Biomacromolecules 11(8):2000–2007. doi:10.1021/bm100366h
31. Suchy M, Hakala T, Kangas H, Kontturi E, Tammelin T, Pursula T, Vuorinen T (2009) Effects of commercial cellobiohydrolase treatment on fiber strength and morphology of bleached hardwood pulp. Holzforschung 63:731–736. doi:10.1515/HF.2009.104
32. Terziev N, Daniel G, Marklund A (2005) Dislocations in Norway spruce fibres and their effect on properties of pulp and paper. Holzforschung 59:163–179
33. Thygesen LG (2008) Quantification of dislocations in hemp fibers using acid hydrolysis and fiber segment length distributions. J Mater Sci 43:1311–1317. doi:10.1007/s10853-007-2284-4
34. Thygesen LG, Asgharipour M (2008) The effects of growth and storage conditions on dislocations in hemp fibres. J Mater Sci 43:3670–3673. doi:10.1007/s10853-008-2587
35. Thygesen LG, Bilde-Sørensen JB, Hoffmeyer P (2006) Visualisation of dislocations in hemp fibres: a comparison between scanning electron microscopy (SEM) and polarized light microscopy (PLM). Ind Crop Prod 24:181–185. doi:10.1016/j.indcrop.2006.03.009
36. Thygesen LG, Eder M, Burgert I (2007) Dislocations in single hemp fibres—investigations into the relationship of structural distortions and tensile properties at the cell wall level. J Mater Sci 42:558–564. doi:10.1007/s10853-006-1113-5